Approximating Rapid Pyrolysis of Coal Particles with Shrinking Core Model

Mohammad R. Hajaligol and Sung C. Yi
Philip Morris U.S.A.
Research Center, P.O.Box 26583
Richmond, Va 23112

INTRODUCTION

Coal pyrolysis is a complex phenomenon and when it is accompanied with rapid heating conditions, it becomes even more complex. A robust but mathematically simple approach is needed when such complexities are encountered. Literature on coal pyrolysis modeling are extensive. Part of this literature describes empirical approaches(1-2), while others include phenomenological and/or physico-chemical approaches (3-6) toward modelling this complex system. Due to these complexities the outcomes of the models appear to be more of a mathematical correlation than mechanistic relations. Accurate knowledge of pyrolysis temperature is one of the essentials in these studies. This becomes more dominant when heating rates approach extremely high values. According to Hajaligol et al. (7,8) and others (2,9,15), at lower heating rates, pyrolysis occurs volumetrically and there exist conditions where pyrolysis is controlled by chemical kinetics. With higher heating rates pyrolysis becomes controlled by heat transfer to the particle that eventually enters an ablation regime (9). On the other hand there are indications that pyrolysis kinetics is influenced by heating rate (11). Since pyrolysis occurs at higher temperatures for higher heating rates, the mechanism of reaction might have been altered. These complexities have led some investigators to believe that pyrolysis has to be explained with a scheme different than chemical reactions (12).

The focus of this study is to show that for high heating rates (> 10^5 K/s), pyrolysis in a particle occurs according to a shrinking core model rather than a volumetric model in which temperature gradient is the driving force. Quite simply it is shown that temperature at pyrolysis front is different than that of particle surface temperature under this extreme heating condition. This temperature is uniquely dependent upon the pyrolysis kinetics, but not on the external heating conditions nor on the thermal properties of the particle. This study provides information on the primary pyrolysis kinetics of coal which can be estimated under these heating conditions.

MATHEMATICAL ANALYSIS

Pyrolysis is modelled for a single spherical coal particle which is pyrolyzed via a single first-order reaction with Arrehenius kinetics

$$\frac{dV}{dt} = (V^* - V)k_0 EXP(-E/RT) \tag{1}$$

Thermophysical properties of the particle can be constant or variable and depend on the temperature. Heat is transmitted into the particle by conduction. Other modes of heat transfer are shown to be less significant under these heating conditions. A standard heat balance on

the particle leads to the following governing partial differential equations

$$\rho C_p \frac{\partial T}{\partial t} = \frac{1}{r^2}\frac{\partial}{\partial r}(r^2 \lambda \frac{\partial T}{\partial r}) - \rho u C_p \frac{\partial T}{\partial r} + (-\Delta H)\rho(V^* - V)k_o EXP(-E/RT) \tag{2}$$

$$\frac{\partial \rho}{\partial t} = -\frac{1}{r^2}\frac{\partial}{\partial r}(r^2 \rho u) + \rho(V^* - V)k_o EXP(-E/RT) \tag{2a}$$

Equation (2) is solved numerically for the particle temperature field with following initial and boundary conditions. The initial condition is a uniform temperature, T_o, throughout the particle

$$T = T_o \text{ for } t \leq 0 \text{ and all } r \tag{3a}$$

The first boundary condition is the mathematical expression for center-line symmetry of the particle temperature field

$$\frac{\partial T}{\partial r} = 0 \text{ at } r = 0 \text{ for all } t \tag{3b}$$

Second boundary condition can be chosen as a heating rate condition greater than 10^5 K/s or a heat flux density greater than 100 watt at the surface to a desired final temperature as follows:

case a)

$$T = T_o + mt \quad \text{at } r = R_p,\ t \leq t_1$$
$$T = T_s \quad \text{at } r = R_p,\ t > t_1 \tag{3c}$$

case b)

$$-\lambda \frac{\partial T}{\partial r} = q \quad \text{at } r = R_p,\ t \leq t_1$$
$$T = T_s \quad \text{at } r = R_p,\ t > t_1 \tag{3d}$$

The solution to Equation (2) is prediction of the temperature field throughout the particle. This information is then used to compute the instantaneous conversion at any given point to monitor, (i) the pyrolysis front within the particle (points of > 98% conversion) (ii) the temperature where 98 % of conversion has been reached at that point, and (iii) the particle fractional conversion and the total pyrolysis time for the conversion.

RESULTS AND DISCUSSION

Either boundary condition prescribed by a heat flux density (3d) or a surface heating rate (3c) to provide a surface heating time of 1 ms. is used in the above analysis to predict pyrolysis behavior under these thermal conditions. Unless stated, the following numerical values were used for the analysis: ρ=1.3g/cm^3, λ=0.0006 cal/cm-s-K, C_p=0.4cal/g-K, ΔH=1000cal/g, k_o= 10^{13} sec^{-1}, and E=50Kcal/mole.

Figure 1 shows the effects of pyrolysis time on the radial position, and the shape of the pyrolysis front for a 100 μm diameter particle. It clearly demonstrates that under these heating conditions the region

where 98 % conversion has occurred is confined in a thin layer which moves inward with a velocity that depends on the thermo-chemical properties of the particle and external heating loads imposed on the particle. Figure 2 presents the effects of different surface temperatures for a given pyrolysis time on the shape and position of the pyrolysis front. As expected, the higher the surface temperature, the larger the driving force (ΔT), thus the higher the velocity of a pyrolysis front and the shorter the pyrolysis time. Figure 2 also shows that the shape of the pyrolysis front (region with 98 % conversion) does not change with the surface temperature. This is true unless the surface temperature drops below a threshold value.

Results from Figures 1, 2 as well as results for other particle diameters (up to 2 mm) show that regardless of the position of pyrolysis front, particle diameter and surface temperature, the temperature of the pyrolysis front is constant. As will be discussed further, when thermal properties of the particle were changed (λ, ΔH, etc.) or variable thermal properties were assumed or other heating rates (10^5 K/s) were applied, the temperature at the pyrolysis front (where 98 % conversion is reached) did not change. Analysis shows that this temperature (T_i) is a unique function of pyrolysis kinetics, i.e., if k_o or E were to change, the temperature would change accordingly. This is what we called threshold value for temperature.

All the above observations indicate that the pyrolysis under these circumstances could be approximated by a shrinking unreacted core model. Following Szekly et al. (13), but exchanging heat for mass diffusion in their description leads to

$$t = \left[k_o e^{-\frac{E}{RT_i}} \right]^{-1} p(x) + \frac{R_p^2 \rho \left[C_p (T_i - T_o) + \Delta H \right]}{\lambda (T_s - T_i)} g(x) \qquad (4)$$

where p(x) and g(x) are given elsewhere (13). It can be shown that under rapid heating conditions, the first term on the right hand side (which describes the kinetic effects) is insignificant and thus pyrolysis is controlled by diffusional resistance (second term). In order to observe the validity of this hypothesis, a parametric study was conducted using Equation (2). The pyrolysis time for complete conversion was compared with that of Equation (4). Given T_s, E, k_o, and ΔH, when λ or R_p is varied, pyrolysis time will scale with λ and increase with the square of R_p (Figure 3). As can be seen this matches well with Equation (4). When ΔH or T_s varied, the results from Equation (2) did not match well with what predicted from Equation (4), although they did show the same trend (Figure 4). ΔH in the range of 0 to 1000 cal/g does not have a significant effect on Equation (2). This is due to the fact that under these heating conditions the ratio of heat transmitted into the particle to the heat consumed by the pyrolysis at the front is high. When higher values of ΔH (>10000 cal/g) were examined (a hypothetical case) the pyrolysis time and ΔH correlation would come out the same from both Equations (2) and (4). Part of the heat which is transmitted into the particle will also be used to heat up that part of the particle through which the pyrolysis front will pass, this effect becomes less noticeable with increasing T_s as predicted by Equation (4). Again for the very large T_s or (T_s-T_i) where the portion

of total heat which is needed for sensible heat of particle is very small in comparison to the total heat transmitted into the particle, prediction of Equations (2) and (4) are exactly the same.

As presented above when any combination of E and k_o according to Nsakala et al. (14) were chosen, regardless of T_s, λ, ΔH, R_p, the temperature at the pyrolysis front (T_i) showed a dependency only on k_o and E. Results can be seen in Figure 5 where k_o is constant and T_i increases as E increases. When dimensionless time ($t=\alpha t/R_p^2$) was plotted against the pyrolysis rate constant ($k_o e(-E/RT_i)$), the results fall on a single line for any given T_s (Figure 6). This indicates a unique correlation between pyrolysis kinetics and the total pyrolysis time. This is due to the strong functionality of pyrolysis time with λ and R_p (embedded in dimensionless time) and pyrolysis kinetics as discussed above. Furthermore, the results of pyrolysis time for total conversion are consistent with Essenhigh (10,14) and others. Effects of T_s can be calculated from Figure 4 and presented with families of curves in Figure 6 using T_s as a parameter.

Effects of variable thermal properties were also studied. For instance, if a variable $\lambda(t)=1.226\times10^{-5}[1.3+0.96\times(V/V^*)]^{3.5}T^{1/2}$ was assumed instead of λ=0.006 cal/cm-s-k the total pyrolysis time would have changed only by 10%. This is because the effective thermal conductivity is controlled by the char thermal conductivity (outer layer of pyrolysis front) and that is relatively constant for the temperature range studied (1200 - 1500 K). This effect is even less significant for heat of pyrolysis, as discussed above where ΔH was varied from 0 to 1000 cal/g.

The practical implication of these results is that by measuring pyrolysis time for a given particle diameter and surface temperature, one could use Figure 6 to estimate T_i and k. This T_i and k can be used along with Figure 5 to estimate the kinetic parameters for primary pyrolysis of coal under severe thermal conditions.

CONCLUSIONS

1. For the rapid heating rates (>10^5 K/s), pyrolysis is confined to a thin layer and reaction occurs according to the shrinking core model rather than a volumetric reaction model.
2. Under these heating conditions pyrolysis occurs totally under diffusional limitations (in the ablation regime).
3. Activation energy (E) and thermal conductivity (λ) are the most stringent parameters on pyrolysis followed by heat of reaction and the surface temperature.
4. Temperature at the pyrolysis front is different from the surface temperature and is uniquely correlated to the pyrolysis kinetics.
5. Intrinsic pyrolysis kinetics under these heating conditions can be estimated using results of existing analysis.

ACKNOWLEDGEMENTS

Authors gratefully acknowledge Dr. Bruce Losee and Dr. Sarajini A. Deevi of Philip Morris U.S.A. for their helpful comments.

NOMENCLATURES

C_p	heat capacity, [Cal/g-K]
E	activation energy, [Cal/gmole]
k_o	frequency factor, [1/s]
m	heating rate, [K/s]
g(x),p(x)	conversion functions [-]
q	heat flux density, [Cal/cm^2-s]
r	radius, [cm]
R_c	pyrolysis front, [cm]
R_p	particle radius, [cm]
T	temperature [K]
T_o	initial temperature [K]
T_i	temperature at pyrolysis front [K]
T_s	surface temperature [K]
t	time [s]
u	volatiles velocity [cm/sec]
V	percent weight loss
V^*	ultimate weight loss
ΔH	heat of pyrolysis [Cal/g]
λ	thermal conductivity [Cal/cm-s-K]
ρ	density [g/cm^3]
τ	dimensionless time [-]

REFERENCES

1 Howard, J.B., Chemistry of Coal utilization, 2nd supplementary volume, chapter 12, Elliot M.A., Ed., Wiley-Interscience, NY 1981.
2 Galvalas, G.R., Coal pyrolysis, Elservier Scientific, NY 1982.
3 Solomon, P.R., Hamblen, D.G., Carangelo, R.M., Serio, M.A., and Deshpande G.V., ACS., Div. Fuel Chem. prep., 32(3), 83, 1987.
4 Niksa, S., Combustion and Flame, 66, 111, 1986.
5 Niksa, S., AIChE J.,34, 5, 790, 1988.
6 Suberg, E.M., in Chemistry of Coal Conversion, R. Schlosberg, Ed., 67 Plenum, 1985.
7 Hajaligol, M.R., Peters, W.A. and Howard, J.P., Energy and Fuels, 2, 430, 1988.
8 Hajaligol, M.R., Peters, W.A. and Howard, J.P., to be submitted to AIChE, 1989.
9 Villermaux, J., Antoine B., Lede J., and Soulignac, F., ACS Div. Fuel Chem. prep., 28(5), 390, 1983.
10 Misra M.K., and Essenhigh, R.H., ACS Div. Fuel Chem. prep., 32(2), 59, 1982.
11 Ko, C.H., Sanchez, D.M., Peters, W.A. and Howard, J.P., ACS, Div. Fuel Chem. prep., 33(2), 112, 1988.
12 Hertzberg, M., Zlochower I.A., Conti, R.S. and Cashdollar K.L., ACS Div. Fuel Chem. prep., 32(3), 24, 1987.
13 Szekely, J., Evans, J.W., and Sohn, H.Y., Gas-Solid Reactions, Academic Press, N.Y., 1976.
14 Nsakala N., Essenhigh, R.H., and Walker, P.L., Combustion Sci. Tech., 16, 153, 1977.
15 Wanzl, W., Kabler P., Van Heck K.H., and Junten H., ACS Div. Fuel Chem. prep., 32(3), 125, 1987.

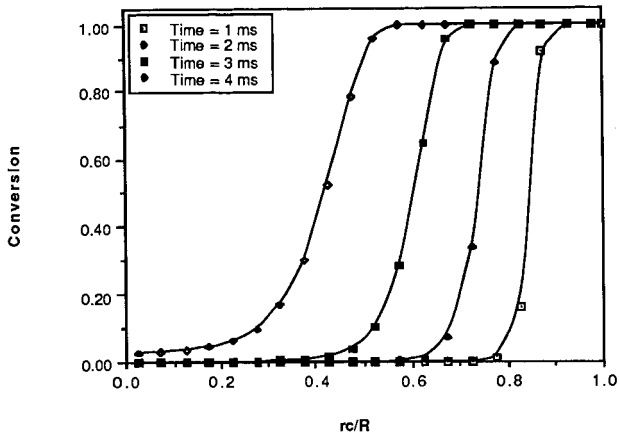

Figure 1. Effect of pyrolysis time on the position and shape of pyrolysis front (T_s=1500 K, R_p=50μm)

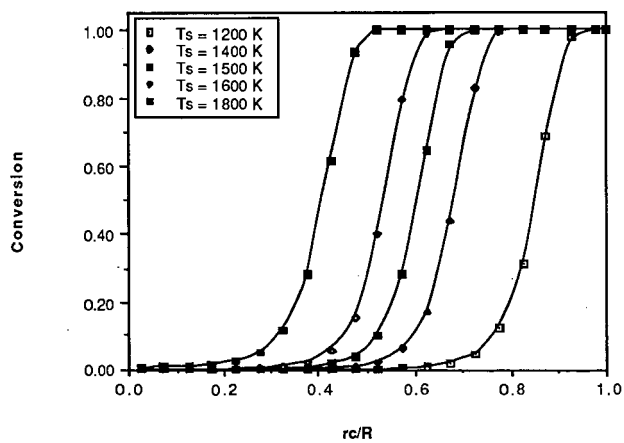

Figure 2. Effect of surface temperature on the position and shape of pyrolysis front (R_p=50μm, 5ms)

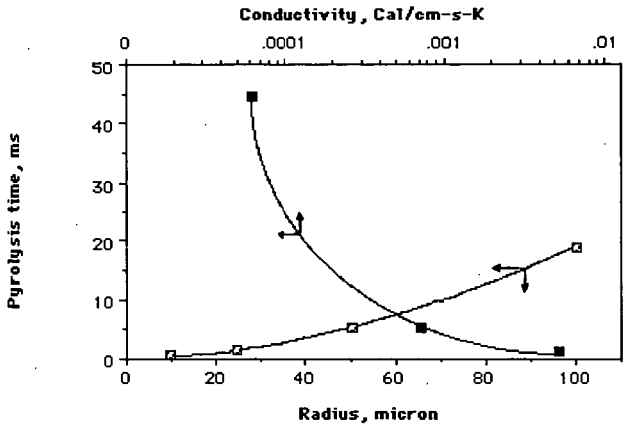

Figure 3. Effect of thermal conductivity and radius on the total pyrolysis time (T_s=1500 K, R_p=50μm)

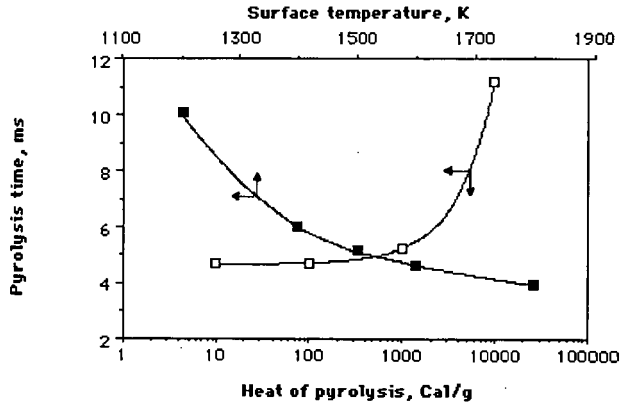

Figure 4. Effect of heat of pyrolysis and surface temperature on the total pyrolysis time (T_s=1500 K, R_p=50μm)

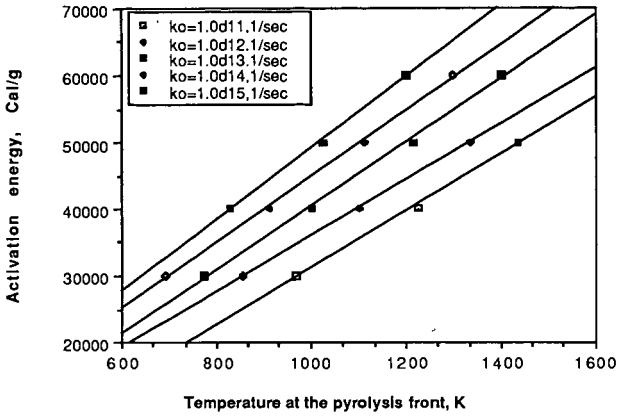

Figure 5. Correlation between activation energy (E), frequency factor (k_o) and the temperature at the pyrolysis front (T_i)

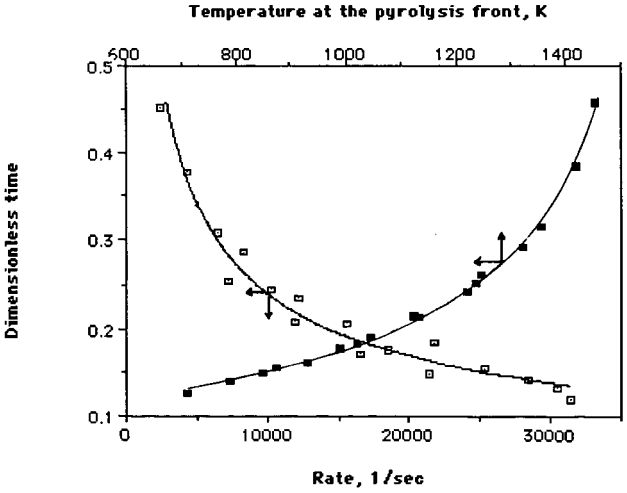

Figure 6. Effect of pyrolysis kinetic and temperature on the pyrolysis dimensionless time